Available online at www.sciencedirect.com
ScienceDirect
Diamond & Related Materials 16 (2007) 2118–2123
DIAMOND AND RELATED MATERIALS
www.elsevier.com/locate/diamond

Differential biocompatibility of carbon nanotubes and nanodiamonds

Amanda M. Schrand [a,b], Liming Dai [a,*], John J. Schlager [b], Saber M. Hussain [b,*], Eiji Osawa [c]

[a] University of Dayton, Department of Chemical and Materials Engineering, 300 College Park, Dayton, OH 45469-0160, USA
[b] Applied Biotechnology Branch, Human Effectiveness Directorate, Air Force Research Laboratory, Wright-Patterson AFB, OH 45433-5707, USA
[c] NanoCarbon Research Institute, Ltd., Kashiwa-no-ha, Kashiwa, Chiba 277-0882, Japan

Available online 2 August 2007

Abstract

Carbon nanomaterials are being produced in increasingly larger quantities for many applications due to their novel characteristics such as enhanced thermal, electrical, mechanical, and biological properties. However, there is a lack of data on biological interactions to assess their biocompatibility before they will be accepted as non-toxic in industrial or biomedical arenas. In the present study, we examined both neuronal and lung cell lines for biocompatibility in aqueous suspensions of carbon nanomaterials, such as nanodiamonds (NDs), single- and multi-walled carbon nanotubes (SWNTs, MWNTs), and carbon black (CB), at concentrations ranging from 25–100 μg/ml for 24 h. Our results indicated that these carbon nanomaterials displayed differential biocompatibility in these two different cell lines. The greatest biocompatibility was found after incubation with NDs and both cell types followed the trend: ND>CB>MWNT>SWNT. Macrophages were found to be more sensitive to the nanomaterials with up to five times the generation of reactive oxygen species after incubation with MWNTs or SWNTs. However, there was a lack of ROS generation from either cell line incubated with ND-raw, as well as intact mitochondrial membranes, suggesting that NDs may be useful as a benchmark nanoparticle non-toxic control in replacement of CB, and should be further investigated for use in medical applications.

Keywords: Carbon nanomaterials; Cell culture; Viability; MTT; MMP; ROS

1. Introduction

Carbon nanomaterials are being produced in increasingly larger quantities for many applications due to their novel characteristics, such as enhanced thermal, electronic, mechanical, and biological properties [1]. In biological systems, they have been used as delivery vehicles [2,3], targeted cancer therapies, tissue scaffolds [4,5], biosensors, and more [6–11]. It is envisaged that nanodiamonds (ND) may be particularly well suited for biological applications that require optical transparency, chemical inertness, hardness, and high specific area [6,12]. Therefore, in view of their biological applications, it is necessary to understand the biocompatibility or toxicity of carbon nanomaterials in either cell-based systems or animal models.

Previous studies in our AFRL laboratory with *in vitro* cell culture models (macrophages, germ-line stem cells, liver cells, PC-12 cells) have shown that nanoparticles can induce size, composition, and concentration-dependent toxicity [13–18]. These same factors are likely to influence carbon nanomaterials' biocompatibility or toxicity. Recent studies suggest that the biocompatibility of carbon-based nanomaterials depends strongly on mass, purity, aspect ratio, and surface functional groups. Jia et al., found that low mass and pure fullerenes (C_{60}, >99.9% purity) were more biocompatible than higher mass and less pure multi-walled carbon nanotubes (MWNT, >95% purity) or single-walled carbon nanotubes (SWNT, >90% purity) in guinea pig alveolar macrophages [19]. Magrez et al., found that human lung tumor cell lines were more biocompatible with high aspect ratio MWNTs than compared to carbon nanofibers (CNF) or carbon black (CB) with lower aspect ratios, while acid functionalization increases the toxicity of both CNF and MWNT [20]. The changes in biocompatibility of these carbon nanomaterials, in relation to size or surface chemistry, can be explained by the high density of reactive bonds on carbon black and carbon

* Corresponding authors. Dai is to be contacted at University of Dayton, Department of Chemical and Materials Engineering, 300 College Park, Dayton OH 45469-0240, United States. Tel.: +1 937 229 2670; fax: +1 937 229 3433. Hussain, Applied Biotechnology Branch, Human Effectiveness Directorate, AFRL/HEPB, 2729 R Street, Bldg 837, Wright-Patterson AFB, OH, 45433-5707, United States. Tel.: +1 937 904 9517; fax: +1 937 904 9610.
E-mail addresses: ldai@udayton.edu (L. Dai), saber.hussain@wpafb.af.mil (S.M. Hussain).

0925-9635/$ - see front matter © 2007 Elsevier B.V. All rights reserved.
doi:10.1016/j.diamond.2007.07.020

nanofibers compared to MWNT [20]. One study using relatively large synthetic abrasive diamond powders (100 nm) (that were electron-beam irradiated and annealed for fluorescence, then incubated with kidney cells for 3 h at a concentration of 400 μg/ml) showed very low cytotoxicity for the diamond nanoparticles after they were internalized by the cells [7]. Our work with much smaller 2–10 nm acid or base-purified nanodiamonds at concentrations of up to 100 μg/ml for 24 h shows high biocompatibility in N2A cells [21]. Together these studies suggest that many factors contribute to the biocompatibility of carbon nanotubes while much less is known about the biocompatibility of NDs. Many studies have examined the biocompatibility of diamond surfaces [22,23], but simple extrapolation of surface biocompatibility data to diamond nanoparticles in solution has been shown to be impossible [9,24].

Other studies that have used *in vitro* cell culture models focused on lung or skin cells due to the risk of exposure in occupational or commercial settings [25–27]. However, it is unclear whether these nanomaterials can reach the nerves associated with these organs either through internalization through the skin and contact with olfactory nerves or translocation across the blood-brain barrier. In the present study, we examined both neuronal (neuroblastoma) and lung (alveolar macrophage) cell lines for biocompatibility in aqueous suspensions of carbon nanomaterials (*e.g.* ND, SWNT, MWNT, CB) at concentrations ranging from 25–100 μg/ml for 24 h. We further examined the morphological and subcellular effects of these nanomaterials on mitochondrial membrane permeability and reactive oxygen species (ROS) generation.

2. Materials and methods

2.1. Nanomaterials characterization

Multi-walled carbon nanotubes (MWNTs) were purchased from Tsinghua University, Beijing, China while single-walled nanotubes (SWNTs) were received from Rice University. Nano-sized carbon black was from Cabot (CB) and micron-sized cadmium oxide (CdO) was from the Fluka Chemical Company. Nanodiamonds (NDs) were generously supplied by NanoCarbon Research Institute Ltd. in Japan and were synthesized according to previously reported detonation techniques [28,29]. Nanomaterials were UV-sterilized, then diluted to stock concentrations of 1 mg/ml in deionized water. Characterization of the carbon nanomaterials size and morphology was performed with transmission electron microscopy (TEM) on a Hitachi H-7600 instrument. Purity was analyzed with inductively-coupled plasma-optical emission spectroscopy (ICP-OES) on a Thermo-Elemental IRIS Advantage ICP.

2.2. Cell culture protocols

Neuroblastoma cells, a neuronal phenotype, were generously provided by Dr. David Cool's laboratory at Wright State University (Dayton, Ohio) and rat alveolar macrophages (NR8383 CRL-2192) were purchased from ATCC (Manassas, VA). Cells were grown in an atmosphere of 5% CO_2 and 37 °C according to standard cell culture techniques [14]. Growth media for the neuroblastoma cells was DMEM/F12 supplemented with 10% normal fetal bovine serum (FBS) and growth media for the macrophages was Ham's Nutrient Mixture F-12K (Kaughn's Modification) media supplemented with 20% FBS. Both medias also contained 1% penicillin–streptomycin (ATCC). Other cell culture supplies included 3-(4,5-dimethylthiazol-2-yl)-2,5-diphenyltetrazolium bromide (MTT, Sigma Chemical Company, St. Louis, MO), 10x Phosphate buffered saline (pH 7.4) and 2.5% trypsin (Gibco Invitrogen™ Corporation, Carlsbad, CA) and rat tail collagen (type 1, UPSTATE, Waltham, MA).

Both neuroblastoma cells and macrophages were seeded in 24-well plates at a concentration of 250,000 cells/ml or approximately 130,000 cells/cm^2 while the plates for macrophages were first coated with type-1 rat tail collagen. After a desired growth period to approximately 80% confluence, cell cultures were dosed with freshly prepared nanoparticle working solutions at a concentration of 25–100 μg/ml in cell culture media without serum for neuroblastoma cells or media with 10% serum for macrophages to reduce proliferation. The 3-[4,5 -thylthiazol-2-yl]-2,5-diphenyl-tetrazolium bromide (MTT) assay was conducted to assess cellular viability based on mitochondrial function [30]. After 30 min of incubation with MTT, a purple color developed within the cells, indicating the cleavage of the tetrazolium salt (MTT) by active mitochondria in live cells. The purple-colored product (formazan crystals) was extracted into solution with acidified isopropanol for homogeneous staining, and the absorbance was measured on a Spectromax 190 microplate reader from 570–630 nm after centrifugation to remove the nanoparticles. The percent reduction of MTT was compared to controls (cells not exposed to nanoparticles), which represented 100% MTT reduction. For fluorescent labeling of mitochondrial membrane permeability, cells were plated at 100,000 cells/ml into 2-chambered slides (Mīt-Σ-Ψ, Biomol). Fluorescence was visualized with TRITC and FITC filters on an Olympus IX71 epifluorescent microscope. Oxidative stress was measured in relation to the generation of reactive oxygen species (ROS). Prior to dosing cells with nanoparticles, the fluorescent probe 2′,7′-dichlorohydrofluorescein diacetate (DCHF-DA, Sigma) was applied under a light controlled environment as described by Wang and Joseph [31]. After nanoparticle treatment, the fluorescent intensity from each well was measured with a 485 nm excitation filter and a 530 nm emission filter on a SpectraMAX Gemini Plus microplate reader (Molecular Devices) equipped with SOFTmax Pro 3.1.2 software (Molecular Devices Corporation). The positive control, hydrogen peroxide (30% H_2O_2, Fisher Scientific), was used to assess the reactivity of the probe and showed a dose-dependent increase in ROS production.

3. Results and discussion

3.1. Nanomaterials characterization

The wide range of primary sizes and shapes of carbon nanomaterials were investigated with transmission electron microscopy (Fig. 1A–D). Individual cubic nanodiamonds (NDs) with sizes ranging from 2–10 nm (Fig. 1A) were smaller than more

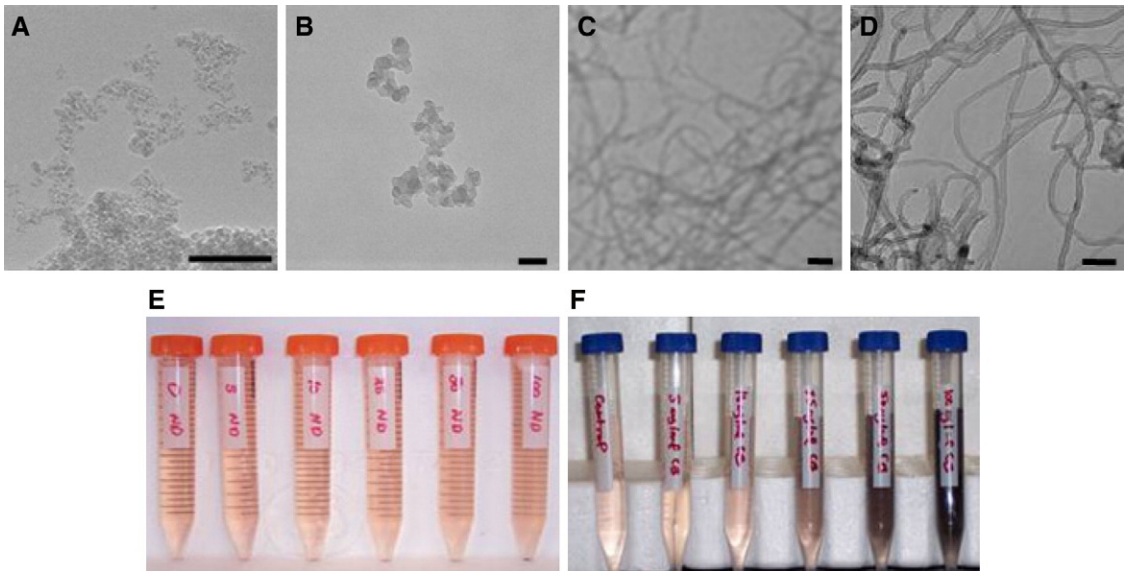

Fig. 1. Characterization of carbon nanomaterials with transmission electron microscopy (TEM) showing sizes and morphologies (A–D) and visualization of nanomaterial solution color and turbidity with increasing concentration (E, F). (A) ND-raw, (B) CB, (C) SWNT bundles, and (D) MWNTs. Scale bars are 100 nm. (E) ND-raw or (F) CB at concentrations of 0, 5, 10, 25, 50, and 100 μg/ml. Note the great difference in color and turbidity between NDs and CB, which was also evident for MWNTs and SWNTs.

spherical fine carbon black (CB) nanoparticles (Fig. 1B) with sizes of approximately 20 nm. Single-walled carbon nanotubes (SWNTs) existed in bundles with diameters up to 25 nm and lengths over 3 μm (Fig. 1C), while multi-walled carbon nanotubes (MWNTs) had diameters ranging from 9–30 nm and lengths up to tens of microns (Fig. 1D). Notice the presence of dark Fe catalyst particles within the MWNT sample (Fig. 1D), which had approximately 0.49 wt.% Fe compared to 0.26 wt.% Fe for the SWNT and no detectable amounts of Fe were found in CB or ND. Additionally, it is clearly evident that the solutions of carbon nanomaterials vary greatly in their color and turbidity, with ND suspensions appearing colorless compared to CB (and nanotube solutions) appearing black in color (Fig. 1E, F). Therefore, the highest concentration used in these studies was limited to 100 μg/ml in order to avoid inhibition of cellular respiration or other processes.

3.2. Morphological examination and assessment of biocompatibility

There is a noticeable difference in internalization between the neuroblastoma cells and macrophages (Fig. 2) after incubation with various carbon nanomaterials for 24 h. As can be seen in Fig. 2, control neuroblastoma cells show neurite extensions (Fig. 2A–E), while macrophages tend to stay round (Fig. 2F–J). The clearly evident phagocytosis of carbon black, completely filling the macrophages and internalization of other carbon nanomaterials (Fig. 2F–J), is markedly contrasted to the neuroblastoma cells (Fig. 2A–E), where clusters of nanomaterials are found attached to the membrane with the internalization not as obvious, showing the differential internalization by these two cell types. In biocompatibility studies, positive, negative, and no-treatment controls are typically used. Multiple methods,

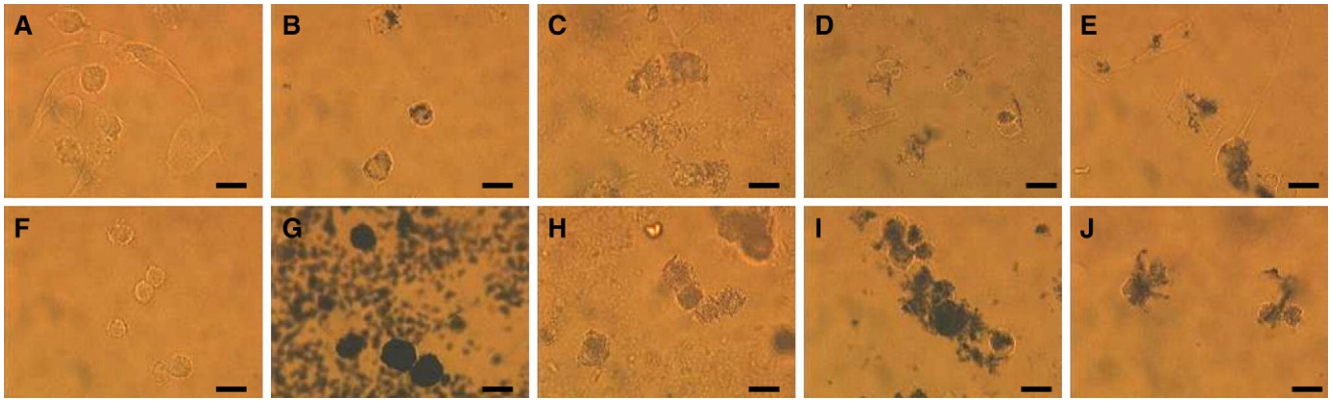

Fig. 2. Phase contrast images of cells (A–E) neuroblastoma and (F–J) macrophage incubated for 24 h with 100 μg/ml of various carbon nanoparticles showing differential uptake. (A, F) Control, (B,G) CB, (C, H) ND-raw, (D, I) MWNTs, and (E, J) SWNTs. Scale bars are 100 μm.

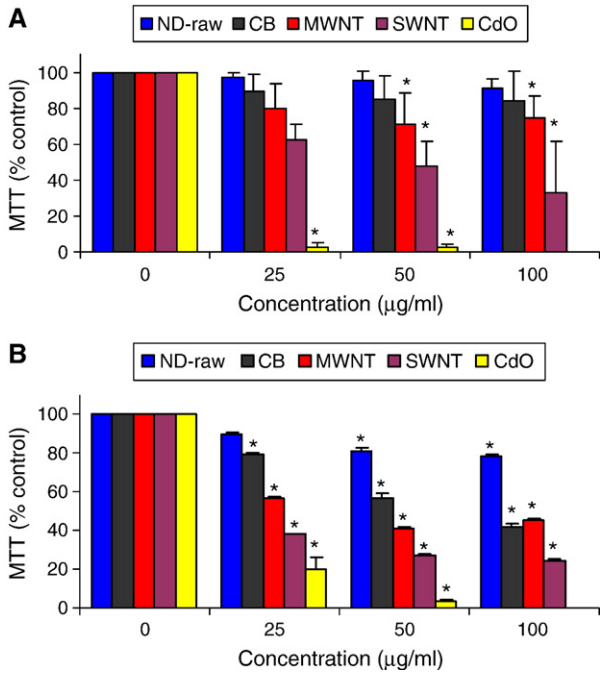

Fig. 3. Cytotoxicity evaluation after 24 h of incubation with various nanocarbons showing differential toxicity due to factors such as nanomaterial composition, size, or shape in (A) neuroblastoma cells or (B) macrophages. Note the similar trends in biocompatibility ND>CB>MWNT>SWNT>CdO for both neuroblastoma cells and macrophages, with the latter being more sensitive to the carbon nanomaterials. Values that were significantly different from the control ($p<0.05$) are denoted with asterisks (*).

such as the MTT assay, mitochondrial membrane permeability (MMP), and generation of reactive oxygen species (ROS), were used to verify the results. The well-known water soluble neurotoxin, cadmium oxide (CdO), was chosen as the positive control. The choice of negative control was a fine carbon black nanoparticle (CB, 20 nm), which has historically been used in inhalation studies as a fine particle control [32]. Both neuroblastoma cells and alveolar macrophages were incubated for 24 h with varying concentrations of carbon nanomaterials and the control materials. The results showed dose-dependent decreases in viability (Fig. 3). For neuroblastoma cells, the interaction with SWNTs and MWNTs significantly decreased viability at concentrations from 50–100 μg/ml, whereas CB did not decrease viability until a concentration of 100 μg/ml (Fig. 3A). In contrast, CdO severely reduced viability at the lowest concentration of 25 μg/ml. The greater decrease in cell viability after exposure to carbon nanotubes compared to CB may explained by the presence of catalysts (*e.g.* Fe). However, the NDs up to the highest concentration of 100 μg/ml did not produce any significant changes in the viability of neuroblastoma cells, presumably suggesting that the purity (presence of catalysts), shapes, and sizes of carbon nanotubes may all contribute to cell damage.

We chose to perform the same MTT assay in alveolar macrophages to test for any cell-type differences in biocompatibility. As shown in Fig. 3B, the macrophages respond to the carbon nanomaterials in a similar manner as the neuroblastoma cells with the greatest biocompatibility for NDs. In both cases, the following general trend of biocompatibility was observed: ND>CB>MWNT>SWNT. However, the decreases in viability were more pronounced for macrophages. There was a significant decrease in viability compared to the control after incubation with carbon-based nanoparticles at concentrations ranging from 25–100 μg/ml, with the exception of ND-raw, which was not significantly different from the control at 25 μg/ml. This suggested cell-specific influences that may contribute

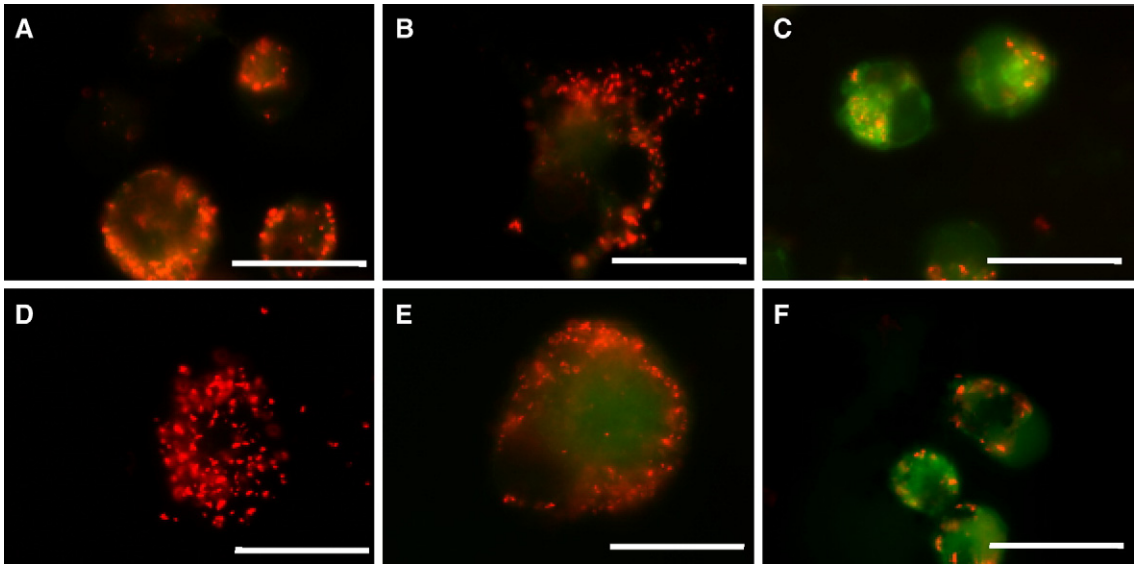

Fig. 4. Mitochondrial membrane permeability assessed with Mīt-Σ-Ψ kit after 24 h of incubation with no treatment (control), positive control CdO, or various carbon nanomaterials. Images A–C are N2A cells and images D–F are macrophages. (A) Control, (B) 100 μg/ml ND-raw, (C) 5 μg/ml CdO, (D) Control, (E) 2.5 μg/ml CdO, and (F) 100 μg/ml MWNT. Note that neuroblastoma cells maintained mitochondrial membrane integrity after incubation with NDs whereas CdO led to leakage and MWNTs caused greater leakage than a low level of CdO in macrophages. Scale bars are 20 μm.

to the differential biocompatibility of the carbon nanomaterials used in these studies include the primary uptake mechanisms of the cells (phagocytosis *vs.* endocytosis) and the inherent ability of these cell types to initiate an inflammatory response or programmed cell death.

The use of a dye (Mīt-Σ-Ψ) to monitor mitochondrial membrane permeability shows that neuronal cells incubated with 100 μg/ml of ND-raw for 24 h retain the red dye similar to control cells, which indicates intact mitochondrial membranes (Fig. 4A–B). However, after neuroblastoma cells were incubated with a 50 μg/ml of CdO, there was leakage from the mitochondrial membranes and dispersion of the dye in a green monomeric form throughout the cytoplasm (Fig. 4C). Examination of macrophages incubated with a lower concentration of CdO (2.5 μg/ml) showed better mitochondrial membrane integrity than cells incubated with 100 μg/ml of MWNTs compared to the control (Fig. 4D–F). This, along with the MTT viability assay, suggests that mitochondrial or apoptotic pathways may be influenced to a much greater extent by the presence of carbon nanotubes or CB than NDs.

Nanomaterials that generate reactive oxygen species (ROS) induce oxidative stress and have been linked to a general toxic response [33]. Although ROS can be natural by-products of cellular redox/enzymatic reactions (*e.g.* mitochondrial respiration, phagocytosis, and metabolism), ROS can also accumulate leading to various pathological conditions [34]. Increases in intracellular ROS represent a potentially toxic insult which, if not neutralized by antioxidant defenses (*e.g.* glutathione and antioxidant enzymes), could lead to membrane dysfunction, protein degradation, and DNA damage [35–39]. We found that carbon nanotubes generated the greatest amount of ROS followed by CB, then ND in both neuroblastoma cells and macrophages (Fig. 5). This trend is correlated with the increased Fe content in MWNT showing higher ROS levels than the SWNT for both cell types. Our results are in agreement with two recent studies where toxicity and the induction of ROS were based on contaminants such as Fe present in carbon nanotubes [40,41]. However, in our study the most noticeable difference between the two cell types was in the amount of ROS produced. The macrophages generated up to five times the amount of ROS compared to neuroblastoma cells after exposure to the same carbon nanomaterials over the same concentration range. Incubation with ND-raw in both cell types did not result in a ROS response, suggesting that the nature of the nanoparticle and/or the associated impurities (*e.g.* Fe) may greatly influence the oxidative stress response of the cells. Acellular assays show that none of the carbon nanomaterials in this study generate ROS in the absence of cells. This fact further implicates the cell-specific response of the macrophages, as immune cells involved in foreign debris clearance in the body, to more readily internalize the carbon nanomaterials used in this study and initiate an inflammatory response in comparison to the neuroblastoma cells. The lack of ROS generation by cells incubated with NDs is consistent with the viability (MTT assay) and mitochondrial membrane integrity (MMP) results over 24 h, indicating an excellent biocompatibility. However, it is not known if the accumulation of nanomaterials inside the cell over longer time periods or at higher concentrations, without their degradation or release, could itself lead to oxidative stress or cell death.

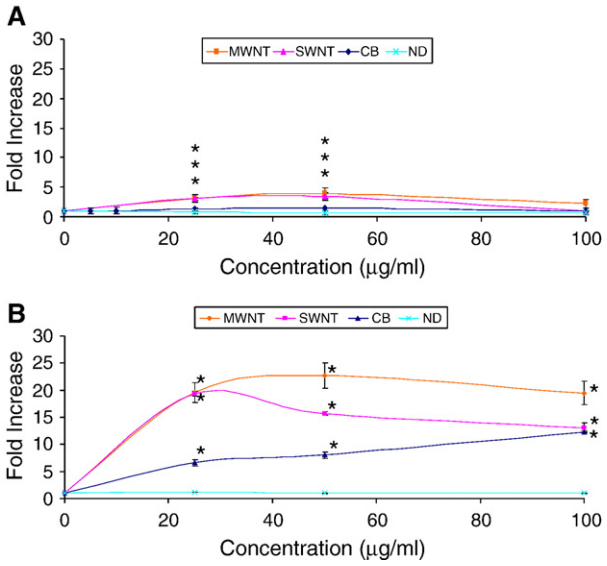

Fig. 5. Generation of reactive oxygen species (ROS) determined by the hydrolysis of DCFH-DA after 24 h of incubation with various carbon nanomaterials in (A) neuroblastoma cells and (B) macrophages. Note that macrophages produce approximately five times the ROS when exposed to the same nanomaterials at the same concentrations as neuroblastoma cells. All values were significantly different from the control ($p<0.05$) with the exception of the NDs (A, B) and 100 μg/ml concentrations in (A).

4. Conclusions

In the present study, we found that NDs were more biocompatible than CB, MWNTs, or SWNTs, respectively, in two different cell types (neuroblastoma and alveolar macrophage), though macrophages are more sensitive to the carbon nanomaterials likely due to their innate response to foreign materials. Examination of the cell morphologies revealed that neuroblastoma cells can lose their neurite extensions after incubation with carbon nanomaterials at high (100 μg/ml) concentrations, whereas macrophages increase in size due to nanomaterial accumulation, but remain round. NDs do not disrupt the mitochondrial membrane and lack ROS, while carbon nanotubes can cause membrane leakage and generate ROS. On the basis of these results, one immediate suggested application of NDs in biocompatibility studies would be as a replacement for the fine CB presently used in some studies as a negative nanoparticle control.

Acknowledgments

The authors thank Col J. Riddle of AFRL/HEPB for his strong support and encouragement for this research and the Nanoscale Engineering Science & Technology (NEST) Laboratory at the University of Dayton for use of TEM. Ms. Amanda Schrand is funded by the Biosciences and Protection Division, Air Force Research Laboratory under the Oak Ridge Institute for Science and Education, Oak Ridge TN. Ms. Schrand is also

funded by the Dayton Area Graduate Studies Institute (DAGSI). L.D. and E.O. thank NEDO (04IT4) for financial support.

References

[1] L. Dai (Ed.), Carbon Nanotechnology: Recent Developments in Chemistry, Physics, Materials Science and Device Applications, Elsevier, Amsterdam, 2006.
[2] A. Bianco, K. Kostarelos, C.D. Partidos, M. Prato, Chem. Commun. (2005) 571.
[3] N.W.S. Kam, T.C. Jessop, P.A. Wender, H. Dai, J. Am. Chem. Soc. 126 (2004) 6850.
[4] V. Lovat, D. Pantarotto, L. Lagostena, B. Cacciari, M. Grandolfo, M. Righi, G. Spalluto, M. Prato, L. Ballerini, Nano Lett. 5 (2005) 1107.
[5] H. Hu, Y. Ni, V. Montana, R.C. Haddon, V. Parpura, Nano Lett. 4 (2004) 507.
[6] L.-C.L. Huang, H.-C. Chang, Langmuir 20 (2004) 5879.
[7] S.-J. Yu, M.-W. Kang, H.-C. Chang, K.-M. Chen, Y.-C. Yu, J. Am. Chem. Soc. 127 (2005) 17604.
[8] W. Yang, O. Auciello, J.E. Butler, W. Cai, J.A. Carlisle, J.E. Gerbi, D.M. Gruen, T. Knickerbocker, T.L. Lasseter, J.R. Russell Jr., L.M. Smith, R.J. Hamers, Nat. Matters 1 (2002) 253.
[9] W.C. Poh, K.P. Loh, W.D. Zhang, S. Triparthy, J.-S. Ye, F.-S. Sheu, Langmuir 20 (2004) 5484.
[10] S. Bondar, I.O. Pozdnyakova, A.P. Puzyr, Phys. Solid State 46 (2004) 758.
[11] D. Pantarotto, J.-P. Briand, M. Prato, A. Bianco, Chem. Commun. (2004) 16.
[12] O.A. Shenderova, V.V. Zhirnov, D.W. Brenner, Crit. Rev. Solid State Mater. Sci. 27 (2002) 227.
[13] S. Trohalaki, R.J. Zellmer, R. Pachter, S.M. Hussain, J.M. Frazier, Toxicol. Sci. 68 (2002) 498.
[14] S.M. Hussain, J.M. Frazier, Toxicol. Sci. 69 (2002) 424.
[15] S.M. Hussain, J.M. Frazier, Toxicol. In Vitro 17 (2003) 343.
[16] S.M. Hussain, K.L. Hess, J.M. Gearhart, K.T. Geiss, J.J. Schlager, J. Toxicol. In Vitro 19 (2005) 975.
[17] S.M. Hussain, A.K. Javorina, A.M. Schrand, H.M. Duhart, S.F. Ali, J.J. Schlager, Toxicol. Sci. 92 (2006) 456.
[18] L. Braydich-Stolle, S. Hussain, J.J. Schlager, M. Hofmann, Toxicol. Sci. 88 (2005) 412.
[19] G. Jia, H. Wang, L. Yan, X. Wang, R. Pei, T. Yan, Y. Zhao, X. Guo, Environ. Sci. Technol. 39 (2005) 1378.
[20] A. Magrez, S. Kasas, V. Salicio, N. Pasquier, J.-W. Seo, M. Celio, S. Catsicas, B. Schwaller, L. Forro, Nano Lett. 6 (2006) 1121.
[21] A.M. Schrand, H. Huang, C. Carlson, J.J. Schlager, E. Osawa, S.M. Hussain, L. Dai, J. Phys. Chem., B 111 (1) (2007) 2.
[22] P. Ariano, P. Baldelli, E. Carbone, A. Gilardino, A.-L. Giudice, D. Lovisolo, C. Manfredotti, M. Novara, H. Sternscheulte, E. Vittone, Diam. Relat. Mater. 14 (2005) 669.
[23] W. Okrój, M. Kamiñska, L. Klimek, W. Szymañski, B. Walkowiak, Diam. Relat. Mater. 15 (2006) 1535.
[24] T.S. Huang, Y. Tzeng, Y.K. Liu, Y.C. Chen, K.R. Walker, R. Guntupalli, C. Liu, Diam. Relat. Mater. 13 (2004) 1098.
[25] N.A. Monteiro-Riviere, A.O. Inman, Carbon 44 (2006) 1070.
[26] K. Soto, A. Carrasco, T. Powell, K. Garza, L. Murr, J. Nanopart. Res. 7 (2005) 145.
[27] S. Fiorito, A. Serafino, F. Andreola, P. Bernier, Carbon 44 (2006) 1100.
[28] A. Krüger, F. Kataoka, M. Ozawa, T. Fujino, Y. Suzuki, A.E. Aleksenskii, A. Ya. Vul', E. Ōsawa, Carbon 43 (2005) 1722.
[29] N.R. Greiner, D.S. Phillips, J.D. Johnson, F. Volk, Nature 333 (1988) 440.
[30] J. Carmichael, W.G. DeGraff, A.F. Gazdar, J.D. Minna, J.B. Mitchell, J. Cancer Res. 47 (1987) 936.
[31] H. Wang, J.A. Joseph, Free Radic. Biol. Med. 27 (1999) 612.
[32] A.A. Shvedova, E.R. Kisin, R. Mercer, A.R. Murray, V.J. Johnson, A.I. Potapovich, Y.Y. Tyurina, O. Gorelik, S. Arepalli, D. Schwegler-Berry, A.F. Hubbs, J. Antonini, Am. J. Physiol., Lung Cell. Mol. Physiol. 289 (2005) L698.
[33] A. Nel, T. Xia, L. Madler, N. Li, Science 311 (2006) 622.
[34] J.L. Farber, M.E. Kyle, J.B. Coleman, Lab. Invest. 62 (1990) 670.
[35] N.E. Preece, J.A. Timbrell, Pharmacol. Toxicol. 64 (1989) 282.
[36] S. Loft, H.E. Poulsen, Methods Enzymol. 300 (1999) 166.
[37] B. Halliwell, J.M. Gutteridge, C.E. Cross, J. Lab. Clin. Med. 119 (1992) 598.
[38] B.P Yu, Physiol. Rev. 74 (1994) 139.
[39] B.K. Siesjo, C.D. Agardh, F. Bengtsson, Cerebrovasc. Brain Metab. Rev. 1 (1989) 165.
[40] V.E. Kagan, Y.Y. Tyurina, V.A. Tyurin, N.V. Konduru, A.I. Potapovich, A.N. Osipov, E.R. Kisin, D. Schwegler-Berry, R. Mercer, V. Castranova, A.A. Shvedova, Toxicol. Lett. 165 (2006) 88.
[41] K. Pulskamp, s. Diabaté, H.F. Krug, Toxicol. Lett. 168 (2007) 58.